Journal of Biomedical Optics

BiomedicalOptics.SPIEDigitalLibrary.org

In vivo three-dimensional imaging of human corneal nerves using Fourier-domain optical coherence tomography

Jun Geun Shin
Ho Sik Hwang
Tae Joong Eom
Byeong Ha Lee

SPIE.

Jun Geun Shin, Ho Sik Hwang, Tae Joong Eom, Byeong Ha Lee, "*In vivo* three-dimensional imaging of human corneal nerves using Fourier-domain optical coherence tomography," *J. Biomed. Opt.* **22**(1), 010501 (2017), doi: 10.1117/1.JBO.22.1.010501.

In vivo three-dimensional imaging of human corneal nerves using Fourier-domain optical coherence tomography

Jun Geun Shin,[a] Ho Sik Hwang,[b] Tae Joong Eom,[c,*] and Byeong Ha Lee[a,*]

[a]Gwangju Institute of Science and Technology, School of Electrical Engineering and Computer Science, 123 Cheomdan-gwagiro, Gwangju 61005, Republic of Korea

[b]Hallym University, Chuncheon Sacred Heart Hospital College of Medicine, Department of Ophthalmology, 153 Gyo-dong, Chuncheon 24253, Republic of Korea

[c]Gwangju Institute of Science and Technology, Advanced Photonic Research Institute, 123 Cheomdan-gwagiro, Gwangju 61005, Republic of Korea

Abstract. We have employed Fourier-domain optical coherence tomography (FD-OCT) to achieve corneal nerve imaging, which could be useful in surgical planning and refractive surgery. Because the three-dimensional (3-D) images of the corneal nerves were acquired *in vivo*, unintentional movement of the subject during the measurement led to imaging artifacts. These artifacts were compensated for with a series of signal processing techniques, namely realigning A-scan images to flatten the boundary and cross-correlating adjacent B-scan images. To overcome the undesirably large signal from scattering at the corneal surface and iris, volume rendering and maximum intensity projections were performed with only the data taken in the stromal region of the cornea, which is located between 200 and 500 μm from the corneal surface. The 3-D volume imaging of a 10×10 mm^2 area took 9.8 s, which is slightly shorter than the normal tear breakup time. This allowed us to image the branched and threadlike corneal nerve bundles within the human eye. The experimental results show that FD-OCT systems have the potential to be useful in clinical investigations of corneal nerves and by minimizing nerve injury during clinical or surgical procedures. [DOI: 10.1117/1.JBO.22.1.010501]

Keywords: corneal nerve; optical coherence tomography; image processing; medical imaging; biomedical optics.

Paper 160619LR received Sep. 10, 2016; accepted for publication Dec. 7, 2016; published online Jan. 5, 2017.

Human corneas have a high density of nerves,[1] which play a significant role in tear production/secretion, the blink reflex, and wound healing.[2] Corneal nerves help to maintain healthy ocular surfaces due to their trophic influence on the corneal epithelium.[3] However, these nerves are routinely injured by refractive surgical procedures, cataract surgeries, and various corneal diseases.[4–6] This damage may lead to several problems, including chronic neurotrophic defects and dry eye syndrome.[3]

Because corneal nerve functions are so important, imaging of these nerves has been attempted in various ways. In the case of *in vitro* imaging, one normally uses an optical or electron microscope with stained corneas.[7] However, although the *in vitro* observations might be good for research and investigation, they are not very clinically useful. In clinical trials, corneal nerves are generally observed with a slit lamp microscope, but this gives only limited cross-sectional information. Figure 1(a) shows a photograph of an anterior segment of a human eye taken with a slit lamp microscope, showing a stromal corneal nerve. Alternatively, images of the corneal subbasal nerve plexus and stromal nerves can be obtained using *in vivo* confocal microscopy (IVCM),[8] but in general this technique allows only for examination of small areas, no larger than 400×400 μm^2. Figure 1(b) shows an IVCM image of a human cornea, taken at a depth of 200 μm from the corneal surface with an imaged area of 340×340 μm^2.

Fourier-domain optical coherence tomography (FD-OCT) provides cross-sectional (2-D) and three-dimensional (3-D) images of a biomedical subject in a noninvasive, noncontact, and label-free manner.[10] Because of these advantages, FD-OCT has been used in presurgical planning and postsurgical evaluation of corneas in refractive surgeries[11] and also in image-guided cataract surgeries.[12] Thus, the clinical applicability of FD-OCT lends corneal nerve imaging the potential to minimize nerve injury during clinical or surgical procedures and to assess the condition of the corneal nerves after clinical surgery or during recovery from disease. Hwang et al.[13] showed that it was possible to image human corneal nerves with 3-D OCT. Their work revealed that several challenges need to be overcome to achieve effective visualization of human stromal corneal nerves *in vivo*. First, nerves are very thin: the mean diameter of a nerve bundle is 20.3 ± 7.0 μm.[7] Thus, very precise motion compensation is needed to correctly visualize the nerves. The involuntary motion of the subject during data acquisition introduces distortions and artifacts, which makes it impossible to even identify the corneal nerves in OCT images. The human cornea has many keratocytes, which are evenly distributed inside the cornea and has cross-sectional areas[14] of 77.7 to 210.6 μm^2 with a mean of 151.1 ± 29.8 μm^2. The white dots in Fig. 1(b) taken with IVCM are keratocyte nuclei, which also appear frequently in OCT images.[15] Sometimes the randomly distributed keratocytes are imaged like a speckle pattern in an OCT image. Importantly, clinicians should ensure that subjects do not blink their eyes or experience tear breakup during the image acquisition process. This requires a fast data acquisition technique, including fast 3-D scanning.

In this paper, we propose some solutions to these open problems in *in vivo* 3-D OCT imaging of human corneal nerves, mainly in the areas of fast data acquisition and effective motion compensation. The system we propose is designed to acquire a 3-D image faster than the normal tear breakup time (TBUT) of a human, which is longer than 10 s and is closely related to spontaneous blinking and pain.[16] The artifacts induced by involuntary motion of the subject during data acquisition are compensated for using a series of signal processing techniques. Specifically, the precise motion compensation technique uses

*Address all correspondence to: Tae Joong Eom, E-mail: eomtj@gist.ac.kr; Byeong Ha Lee, E-mail: leebh@gist.ac.kr

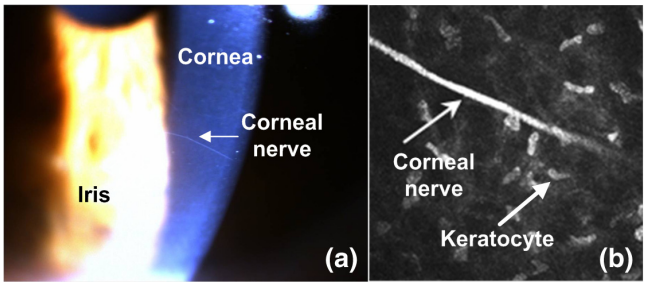

Fig. 1 Images of a human corneal stromal nerve taken with (a) a slit lamp microscope and (b) IVCM, Lagali et al. Reproduced from Ref. 9.

the corneal surface as a reference plane and cross-correlates adjacent B-scan images. To minimize the unwanted signals from the high scattering areas at the corneal and iris surfaces, only the mid stromal region is used in volume rendering and maximum intensity projection (MIP). Finally, we present volume rendering and MIP images of branched and threadlike corneal nerves of a human eye taken *in vivo*.

For this experiment, an FD-OCT system was constructed based on a Mach–Zehnder interferometer, which employed a high-speed wavelength-swept laser (Axsun Technologies, Billerica, Massachusetts) with a center wavelength of 1.31 μm and repetition rate of 50 kHz. A fiber coupler and a circulator were used to guide 90% of the laser output to the sample stage. The average power incident on the sample was kept as low as 10 mW, well below the American National Standards Institute maximum permissible exposure of 15.4 mW [for intrabeam viewing through a 7-mm pupil and exposure times of up to 8 h (Ref. 17)]. The OCT interference signal was detected by a balanced photodetector (PDB460C, Thorlabs, Newton, New Jersey) and 4096 samples were collected, more than enough to see the cornea, via an A-line with a 14-bit high-speed digitizer (PX14400, Signatec Inc., Lockport, Illinois). The spectrum interpolation for resampling to k-space was performed on all A-line data prior to the fast Fourier transform (FFT) process. The scan range was set as wide as 10×10 mm^2 with an interval of 14.29 μm for both A- and B-scans such that one 3-D image was composed of equally spaced 700×700 A-lines. Considering the sweep rate of the 50-kHz laser, the 2-D imaging frame rate was 71.43 fps, and one 3-D volume image was acquired within 9.8 s, which is faster than the normal human TBUT. The objective lens (LSM03, Thorlabs, Newton, New Jersey) had a focal length of 36 mm, which gave a spot size of 21 μm at the focal plane when the input beam was Gaussian with a 4-mm diameter. Thus, the lateral resolution was just enough to allow for visualization of 20-μm-thick nerve bundles. The axial resolution of the system was measured to be 8.8 μm in air.

This study was approved by the Institutional Review Board of the Gwangju Institute of Science and Technology (Approval No. 20160616-HR-23-11-02), and written informed consent was obtained from a total of five healthy subjects prior to conducting the imaging procedure. To obtain the 3-D image of corneal nerve bundles *in vivo*, a subject was positioned on the OCT headrest and asked to gaze into the objective lens of the scanner.

Although the FD-OCT system was designed to have a shorter 3-D scanning time than the TBUT, the 3-D OCT image was still easily affected by the involuntary motion, heartbeat, and breath of the subject. As previously discussed, when movement is present, a system with a depth resolution of 8.8 μm in air and lateral beam spot size of 21 μm was not adequate to image a

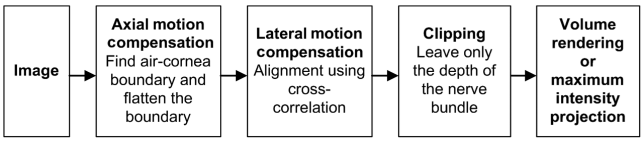

Fig. 2 Flowchart of the signal processing used for visualization of corneal nerves. Axial motion artifacts were compensated for by flattening the corneal surface boundary, and the lateral motion artifacts were dealt with by cross-correlating adjacent B-scan images. To enhance identification of the corneal nerves, the strong signals from the corneal and iris surfaces were removed.

corneal nerve bundle with a ~20-μm thickness. Therefore, a series of image processing techniques, summarized in Fig. 2, were applied to compensate for the involuntary motion of the subject and to enhance visualization of the image.

First, the axial motion artifacts were compensated for by using the top surface of the cornea as the reference plane. For all 2-D (B-scan) OCT image data, the composing A-lines were adjusted so that they had the same flat air-corneal boundary as shown in Fig. 3. The FD-OCT 2-D image of an anterior segment of a human eye shown in Fig. 3(a) was realigned to have a flat corneal surface as in Fig. 3(b). As shown, the corneal nerve bundles can be barely visualized with the assistance of the yellow arrows. To achieve corneal surface flattening, the adjacent A-lines were adjusted by 1.66 ± 3.45 μm. However, among the B-scans, adjustments of up to 26.4 μm were made, mainly due

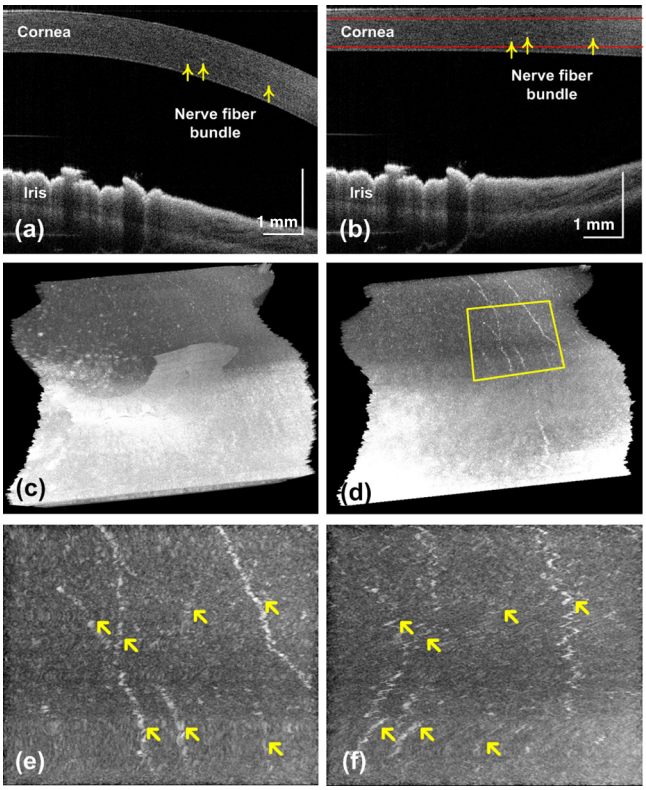

Fig. 3 OCT images of a human cornea (23-year-old male): (a) raw B-scan image, (b) boundary flattened B-scan image, (c) volume image rendered with the motion-compensated data, (d) motion-compensated volume image rendered only with the clipped region of (b) (the area between the red lines), (e) enlarged image of (d) (area in the yellow box), and (f) the same image as (e) taken without lateral motion compensation.

to the axial movement of the subject, in addition to the corneal curvature adjustment of 2437 μm.

Second, images were cross correlated to calculate for lateral motion. When scanning is done at a high density, the internal structure variation is small and adjacent B-scan images become very similar so the cross correlation is high. Therefore, when there was lateral motion between adjacent B-scans, the motion could be calculated by sliding B-scan data from one image over the other and finding the displacement x that gives the maximum cross correlation. In general, the cross-correlation function between the k'th B-scan OCT image and its adjacent $(k+1)$'th image laterally offset by x pixels is given by

$$\varphi(x) = \begin{cases} \frac{1}{N(M-|x|)} \sum_{i=0}^{M-x-1} \sum_{j=0}^{N-1} I_{i,j,k} I_{i,j+x,k+1}, & x \geq 0 \\ \frac{1}{N(M-|x|)} \sum_{i=-x}^{M-1} \sum_{j=0}^{N-1} I_{i,j,k} I_{i,j+x,k+1}, & x < 0 \end{cases}, \quad (1)$$

where $I_{i,j,k}$ is the intensity of the i'th axial point of the j'th A-line in the k'th B-scan image, N is the number of data points in one A-line, and M is the number of A-lines in one B-scan image. This cross-correlation process was effective due to the keratocytes in the cornea. Because the scans had a density of 14.29 μm, keratocytes of area 150 μm^2 were assumed to appear in a similar pattern in adjacent B-scan images. A motion-compensated 3-D image of the cornea is shown in Fig. 3(c). The coastline-like indentation of the image (left and right boundaries) was a result of lateral motion compensation, and the accumulated compensation was as large as 1140 μm. However, the high reflection and scattering at the corneal and iris surfaces greatly hindered visualization and even identification of the corneal nerves. Thus, it was necessary to isolate the nerve bundle region to improve visualization prior to the volume-rendering process. The corneal nerve bundles enter the eye from the corneosclera to the cornea at a mean distance of 293 ± 106 μm from the ocular surface[7] and move from the periphery toward the center.[3] Figure 3(d) shows the motion-compensated 3-D image constructed only with data from the region between the red lines in Fig. 3(b). The enlarged image in Fig. 3(e) clearly shows bundles of threadlike and branched nerves, as indicated by the yellow arrows. For comparison, the same image without lateral motion compensation is presented in Fig. 3(f), which shows that the connectivity of corneal nerves was severely affected by the motion. At some points, identification of the nerves was not even possible without motion compensation.

The entire area of a human cornea could be imaged *in vivo* with two OCT measurements: temporal and nasal. The commonly used MIP images of the cornea are shown in Figs. 4(a) and 4(b). Although the artifacts due to motion have been corrected, the stromal nerves were too thin compared with the imaging range of 10×10 mm^2. Thus, multiscale line detectors[18] and a simple grayscale morphological operator were utilized with the MIP image to enhance its visibility. Figures 4(c) and 4(d) are the same images shown in (a) and (b) that have been image processed to intentionally thicken the nerves. These images clearly show several branched and threadlike corneal nerves distributed in the stromal region.

This study shows that the proposed methodology has the potential to enable human corneal nerve imaging *in vivo* to assess the condition of corneal nerves and/or to minimize nerve injury during various surgical procedures. A more clinically meaningful experiment is currently being designed. The total number of A- and B-scans was adjusted so that the total

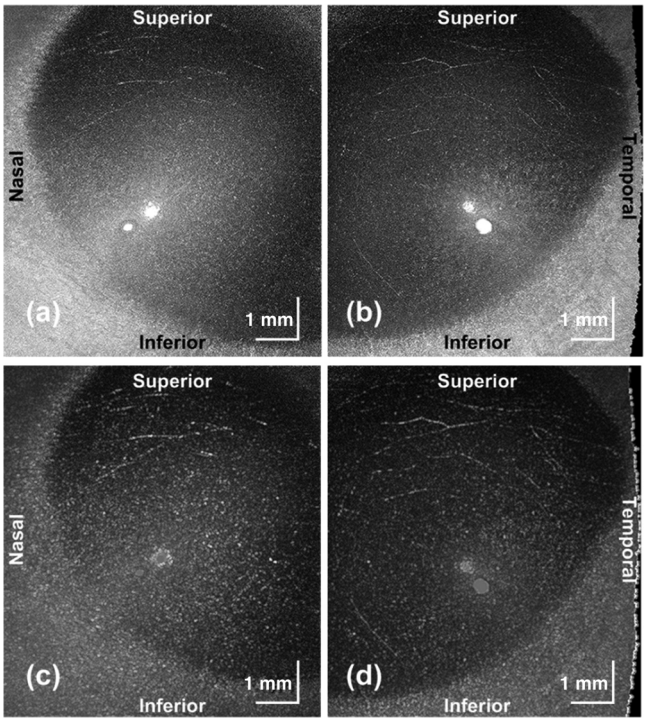

Fig. 4 MIP images of a human cornea (33-year-old male): (a) nasal side and (b) temporal side. To enhance visibility, the nerve images shown in (a) and (b) were intentionally thickened in (c) and (d), respectively.

data acquisition time to obtain one 3-D image became shorter than the TBUT. Because a subject's movement during measurements is a significant problem in clinical applications of the anterior segment of the human eye *in vivo*, imaging with a minimal image acquisition time has been repeatedly attempted.[19,20] In our experiment, the data acquisition time, which was mainly limited by the repetition rate of the laser, was slightly shorter than the normal TBUT. Fortunately, this limitation could be resolved with a high-speed swept laser.[20] With the high-speed data acquisition enabled by this type of laser, we could use a higher numerical aperture (NA) objective lens with a finer scan density, which would increase the lateral resolution of the image and give more detailed information about the corneal stromal nerves distributed over the entire eye. The issues with the short depth of focus of a high NA lens can be reduced by introducing a tunable lens to change the focal point during measurements. The 4096 samples collected per A-line were too many considering the corneal depth of ~3 mm. Although oversampling is beneficial for FFT noise reduction and k-space conversion in general, it should often be reduced when possible to conserve resources in a practical system.

In summary, we have presented 3-D *in vivo* images of human corneal nerves taken with a high-speed FD-OCT system. The data acquisition time for a 10×10 mm^2 anterior segment of the eye was 9.8 s, which is slightly shorter than the normal TBUT. The entire corneal area was imaged with just two FD-OCT measurements. Image distortions due to the subject's motion during measurements were compensated for with a series of signal processing techniques. Axial motion artifacts were compensated for by realigning the A-scan data so the corneal surface image was flat. Lateral motion artifacts were compensated for by cross-correlating adjacent B-scan images.

Although the keratocytes in the cornea hindered visualization of the stromal corneal nerves, they did enable cross correlation, which in turn calculated for lateral motion. The visibility of the corneal nerve fiber bundles was increased by rendering only the stromal region of the cornea. These efforts allowed us to successfully image the bundles of branched and threadlike corneal nerves in a human eye. However, for this technique to be clinically applicable, the data acquisition speed should be increased a little more. The recently released ultrahigh-speed swept source might enable this in the near future.

Disclosures

Authors declare that there are no conflicts of interest regarding the publication of this paper.

Acknowledgments

This work was supported by the GIST Research Institute (GRI) in 2016, the Industrial Technology Innovation Program (No. 10063062), and the Industrial Strategic Technology Development Program (No. 10063364) of the Ministry of Trade, Industry and Energy of Korea, and Basic Science Research Program (No. 2014R1A1A2059210) through the National Research Foundation of Korea (NRF) funded by the Ministry of Education.

References

1. L. J. Müller et al., "Architecture of human corneal nerves," *Invest. Ophthalmol. Vis. Sci.* **38**(5), 985–994 (1997).
2. R. W. Beuerman and B. Schimmelpfennig, "Sensory denervation of the rabbit cornea affects epithelial properties," *Exp. Neurol.* **69**(1), 196–201 (1980).
3. L. J. Müller et al., "Corneal nerves: structure, contents and function," *Exp. Eye Res.* **76**(5), 521–542 (2003).
4. C. Belmonte, "Eye dryness sensations after refractive surgery: Impaired tear secretion or 'phantom' cornea?," *J. Refract. Surg.* **23**(6), 598–602 (2007).
5. A. Cruzat et al., "Inflammation and the nervous system: the connection in the cornea in patients with infectious keratitis," *Invest. Ophthalmol. Vis. Sci.* **52**(8), 5136–5143 (2011).
6. M. Kohlhaas, "Corneal sensation after cataract and refractive surgery," *J. Cataract Refract. Surg.* **24**(10), 1399–1409 (1998).
7. C. F. Marfurt et al., "Anatomy of the human corneal innervation," *Exp. Eye Res.* **90**(4), 478–492 (2010).
8. I. Jalbert et al., "In vivo confocal microscopy of the human cornea," *Br. J. Ophthalmol.* **87**(2), 225–236 (2003).
9. N. Legali et al., "Laser-scanning in vivo confocal microscopy of the cornea: imaging and analysis methods for preclinical and clinical applications," in *Confocal Laser Microscopy–Principles and Applications in Medicine, Biology, and the Food Sciences*, p. 55, InTech (2015).
10. A. F. Fercher et al., "Measurement of intraocular distances by backscattering spectral interferometry," *Opt. Commun.* **117**(1–2), 43–48 (1995).
11. V. Hurmeric, S. H. Yoo, and F. M. Mutlu, "Optical coherence tomography in cornea and refractive surgery," *Expert Rev. Ophthalmol.* **7**(3), 241–250 (2012).
12. E. Donaldson et al., "Femtosecond laser-assisted cataract surgery," *J. Cataract Refract. Surg.* **39**(11), 1753–1763 (2013).
13. H. S. Hwang et al., "Visualization of corneal nerve distribution by 3D optical coherence tomography," *Invest. Ophthalmol. Vis. Sci.* **55**(13), 2462–2462 (2014).
14. I. Prydal et al., "Keratocyte density and size in conscious humans by digital image analysis of confocal images," *Eye* **12**(3a), 337–342 (1998).
15. A.-H. Karimi, A. Wong, and K. Bizheva, "Automated detection and cell density assessment of keratocytes in the human corneal stroma from ultrahigh resolution optical coherence tomograms," *Biomed. Opt. Express* **2**(10), 2905 (2011).
16. M. Al-Abdulmunem, "Relation between tear breakup time and spontaneous blink rate," *Int. Contact Lens Clin.* **26**(5), 117–120 (1999).
17. American National Standards Institute and The Laser Institute of America, *American National Standard for Safe Use of Lasers*, The Laser Institute of America, Orlando, Florida (2007).
18. U. T. V. Nguyen et al., "An effective retinal blood vessel segmentation method using multi-scale line detection," *Pattern Recognit.* **46**(3), 703–715 (2013).
19. M. Gora et al., "Ultra high-speed swept source OCT imaging of the anterior segment of human eye at 200 kHz with adjustable imaging range," *Opt. Express* **17**(17), 14880 (2009).
20. W. Wieser et al., "Multi-megahertz OCT: high quality 3D imaging at 20 million A-scans and 45 GVoxels per second," *Opt. Express* **18**(14), 14685 (2010).